HIGHLY SIDEROPHILE ELEMENT ABUNDANCES IN NAKHLITE AND CHASSIGNITE SULFIDES. Marine Paquet[1], James M. D. Day[1], Arya Udry[2]. [1]Scripps Institution of Oceanography, University of California San Diego, La Jolla CA 92093-0244, USA; email: mpaquet@ucsd.edu, [2]Department of Geosciences, University of Nevada, Las Vegas, 4505 S. Maryland Parkway, Las Vegas, NV 89154, USA.

Introduction: The martian nakhlite and chassignite meteorites are the only coherent genetic suite of rocks from the red planet and provide insights into the composition of the martian mantle and magmatic differentiation processes [1, 2]. Nakhlites and chassignites are likely derived from low degree partial melting of hydrated and metasomatized depleted mantle lithosphere, whereas shergottite melts sample deeper mantle sources [1]. Highly siderophile elements (HSE: Au, Re, Pd, Pt, Rh, Ir, Ru, Os) are sited within sulfide assemblages in shergottites [3, 4], and can be used to address the nature of sulfide fractionation and parental melt compositions for these rocks [5, 6]. To date, only limited HSE data exist for whole-rock nakhlites and chassignites (e.g., [7-9]), and sulfide assemblages in these meteorites have not been characterized. We report siderophile and highly siderophile element abundance for sulfide mineral assemblages within 12 nakhlites and two chassignites (Chassigny, NWA 2737) measured by laser ablation inductively coupled plasma mass spectrometry (LA-ICP-MS) to examine parental melt compositions and sulfide fractionation in these rocks, and to compare them with shergottites.

Samples and Methods: Sulfides were characterized for major- and trace-element compositions (including highly siderophile elements) in 12 nakhlite and two chassignite polished sections (Caleta el Cobre (CeC) 022; Governador Valadares; Lafayette (USNM 1805-8); Miller Range (MIL) 03346; MIL 090030; MIL 090032; MIL 090136; Nakhla (USNM 5891-2); Northwest Africa (NWA) 817; NWA 998; NWA 11013; Yamato (Y) 000749; Chassigny (USNM 624-1); NWA 2737) using a *New Wave* UP-213nm Laser Ablation system coupled to a *Thermo Scientific* iCAP Qc Inductively Coupled Plasma Mass Spectrometer (ICP-MS), following prior work [4]. Where the size of the sulfides were smaller than the laser beam diameter, surrounding silicates were also analyzed for HSE contents to perform a background subtraction. Between seven and fourteen sulfides were measured in each section with the dominant sulfide phase being pyrrhotite (**Fig. 1**).

Results and Discussion: We measured the HSE abundances in sulfide grains occurring in early crystallized silicate phases (olivine, pyroxene) as well as in interstitial sulfide grains, associated with oxides (ilmenite, titanomagnetite). Silicates and oxides have low HSE abundances, typically 10 to 100 lower than the sulfides and often below limits of detection. Measurements done in the mesostasis likely sampled minute sulfide grains, resulting in abundances above detection limits for most of the HSE. Sulfide grains have elevated HSE abundances. The chassignite sulfide population has elevated HSE abundances that are broadly flat on a CI-chondrite normalized plot, with enrichments in Pt and/or Ru. Sulfides in nakhlites have more strongly fractionated HSE patterns and generally lower abundances, with high Re+Pt+Pd relative to Ru+Ir+Os (**Fig. 2**) (with the HSE compatibility for martian magmatism being Os > Ir ≥ Ru >> Pt ≥ Pd ≥ Re; e.g. [6]).

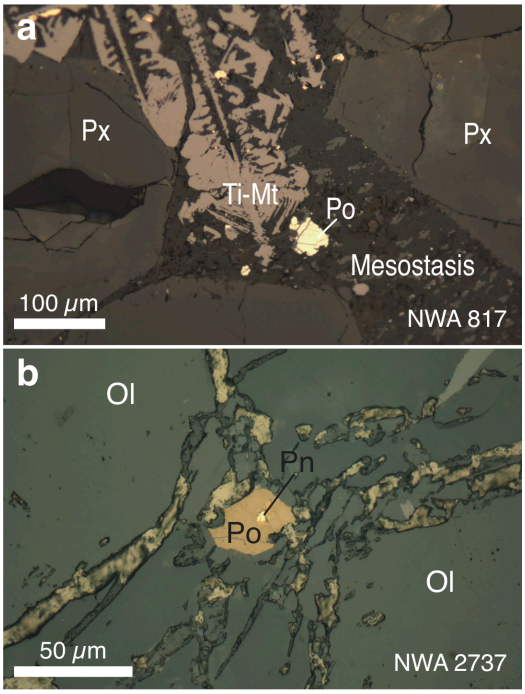

Figure 1. *Sulfide assemblages in NWA 817 and NWA 2737 shown in reflected light. Po = pyrrhotite; Pn = pentlandite; Ti-Mt = titanomagnetite; Px = pyroxene; Ol = olivine.*

Combining HSE abundances measured in the sulfide assemblages of the nakhlites and chassignites with sulfide modal abundances reported by [8], it is possible to estimate HSE bulk compositions for the nakhlites and chassignites (**Fig. 3**), and to compare them to existing whole-rock data for nakhlites [7-9] and shergottites [5,6]. It has previously been demonstrated that chassignites are cumulates from fractional crystallization processes during formation of the nakhlite-chassignite assemblage [1]. The sulfides in the chassignites should, therefore, preserve the HSE compositions closest to parental melt compositions. Fractional crystallization models can therefore be calculated using chassignite

starting compositions, as well as the most primitive enriched and depleted shergottite compositions (**Fig. 3**). Whole-rock data for chassignites appear slightly higher than our HSE estimates from the sulfide compositions, which could be attributed to the contribution of spinel (1.2 to 2.7 modal %, [1]) to the HSE budget of the chassignites, especially for Ru [e.g. 10], or to localized nugget heterogeneity.

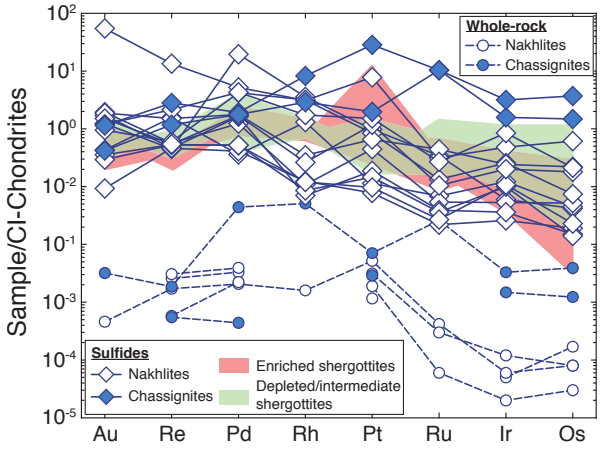

Figure 2. *CI-chondrite normalized HSE patterns for average sulfide compositions in nakhlites and chassignites, compared to sulfide assemblages in depleted, intermediate and enriched shergottites [3], as well as whole-rock data for nakhlites and chassignites [7-9].*

Whereas shergottite compositions are best reproduced by up to 30 to 35% of fractionation of an olivine-dominated cumulate of parent melts with S contents ~200-250 ppm [4], nakhlite HSE compositions can be interpreted in one of two ways. First, assuming a starting composition similar to chassignites, they would have experienced higher degrees of S fractionation of more HSE-depleted melts (between 50 and 55% of the shergottites HSE inventory, and ~150-200 ppm of S). Alternatively, assuming a starting composition similar to shergottite melts, they experienced earlier S fractionation than low MgO shergottites. We favor the first scenario because (1) assuming a shergottite melt initial composition is problematic for explaining the low estimated HSE contents of chassignites; (2) previous work has shown that nakhlites and chassignites derive from low-degree partial melting of a depleted source [2], which would be consistent with the concept of limited HSE from S-saturated melts from an S-poor source.

These characteristics are consistent the highly fractionated HSE patterns observed for the nakhlite sulfide assemblages, compared to the chassignites and shergottites. Moreover, these predictions for high Re/Os in the nakhlites are coherent with existing $^{187}Os/^{188}Os$ ratios [5], and significant S fractionation. Sulfide HSE compositions preserve magmatic signatures and enable assessment of the evolution of the melt composition. Low HSE contents estimated for chassignites are consistent with models of low-degree partial melting of a depleted source on Mars, from which nakhlites are derived by fractionation of olivine-dominated cumulates.

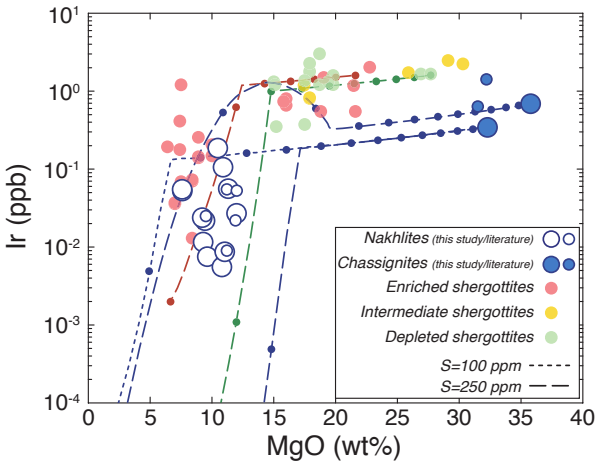

Figure 3*. Estimates for bulk Ir abundances of the nakhlites calculated using the average sulfide compositions and a modal abundance for the sulfides of 0.05% [< 0.01 to 0.05%; 11], bulk rock nakhlite and chassignite data from [7-9] and bulk rock shergottite data from [3, 5] in function of MgO content of the whole rocks. Dotted lines correspond to fractional crystallization models for starting compositions similar to Chassigny and NWA 2737 for the nakhlites, and the most primitive enriched and depleted shergottites, for S contents of 100 ppm and 250 ppm. Partition coefficients are from [6]. The dots correspond to a 5% increment of the fractional crystallization model. For a lower S content in the initial melt, the S-saturation is reached later in the fractionation sequence, leading to an abrupt decrease of the more compatible HSE (Ru, Ir, Os). Note that shergottites have higher bulk HSE compositions (~x100) than the nakhlites and chassignites, due to comparable HSE abundances in the sulfides (Figure 2) but higher sulfide modal abundances (~0.5 to 1% [6, 12, 13]).*

References: [1] Udry, A. & Day, J.M.D. (2018) *GCA*, **238**, 292-315. [2] Day J.M.D. et al. (2018) *Nat. Comm.*, **9**, 4799. [3] Baumgartner R.J. et al. (2017) *GCA*, **210**, 1-24. [4] Paquet M. et al. (2019) *LPSC Abstracts*. [5] Brandon A.D. et al. (2012) *GCA*, **76**, 206-235. [6] Tait K.T. and Day J.M.D. (2018) *EPSL*, **494**, 99-108. [7] Jones J.H. et al. (2003) *Chem Geol*, **196**, 21-41. [8] Dale C.W. et al. (2012) *Science*, **336**, 72-75. [9] Mari, N. et al. (2019) *GCA*, **266**, 416-434. [10] Day, J.M.D. (2013) *Chem Geol*, **341,** 50-74. [11] Chevrier V. et al. (2011) *MAPS*, **46**, 769-784. [12] Basu Sarbadhikari A. et al. (2009) *GCA*, ***73***, 2190-2214. [13] Riches A.J.V. et al. (2011) *Polar Sci.*, ***4(4)***, 497-514.